DOI: 10.15587/978-617-8360-05-4.CH3

Stanislav Sidnei, Mykola Pelypenko,
Grygorian Mykola, Mykhailo Kropyva, Ihor Taran, Serhii Holovchenko


CHAPTER 3

# HIERARCHICAL STRUCTURE OF CALCULATION METHODS FOR ASSESSING THE FIRE RESISTANCE OF ENCLOSURE HORIZONTAL STRUCTURES UNDER THE LIMIT STATE OF LOSS OF INTEGRITY

## ABSTRACT

The paper presents a hierarchical system of calculation methods for assessing the fire resistance of reinforced concrete slabs upon the onset of the limit state of loss of integrity. Three approaches are proposed: tabular, simplified and refined. The tabular method allows to quickly assess the fire resistance of slabs, the simplified method takes into account structural parameters and loads, and the refined method takes into account detailed characteristics of materials and temperature effects for the most accurate results. Such a system provides designers with flexibility during the design phase, allowing them to select the appropriate method depending on the required accuracy and available data. In addition, they help increase the safety of building structures during a fire.

## KEYWORDS

Fire resistance, reinforced concrete slabs, limit state, loss of integrity, tabular method, simplified method, refined method, structural parameters, design, temperature effect of fire.

According to EN 1992-1-2, the hierarchical system of methods for the calculation of reinforced concrete slabs is a structure based on simplified methods, and at the top are refined methods, but only according to the loss of bearing capacity. Since floor slabs and coverings, in addition to the load-bearing function, also perform enclosing functions. They prevent the spread of fire and harmful combustion products that pose a threat to people's lives and health. According to EN 1992-1-2, the conformity of boards to the standardized fire resistance class must be confirmed by three limit states, in particular: loss of load-bearing capacity (*R*), loss of integrity (*E*) or thermal insulation capacity (*I*).

However, according to the results of experimental tests on reinforced concrete floor slabs, it was established that the onset of only the limit state of loss of bearing capacity is taken into account [1]. This is explained by the fact that the onset of the loss of heat-insulating ability occurs much later than the loss of bearing capacity, since concrete is a porous material filled with

air, which is the worst heat conductor among all materials except for vacuum, so the heating of the non-heated surface of such structures to critical temperatures occurs very slowly [2]. For example, in work [3], the maximum temperature on the non-heated side of the slab in a hollow slab for 50 minutes was recorded as only 70 °C min, which indicates its high fire resistance indicators upon the onset of the loss of heat-insulating capacity only, without taking into account the loss of load-bearing capacity and integrity. Thus, the question remains unresolved for floor slabs and coatings, which comes first – loss of bearing capacity or loss of integrity.

Since there are no methods for assessing fire resistance based on the limit state of loss of integrity, and during experiments it is difficult to record the formation of cracks due to covering with loads [3], the calculation approach remains the only option.

In [4–7], it was demonstrated that the limit state of fire resistance, the loss of integrity, occurs earlier than the loss of load-bearing capacity, which creates dangerous conditions during the evacuation of people during a fire and the effective elimination of fires by special units.

Therefore, it is proposed to develop a hierarchical system for assessing fire resistance by loss of integrity of reinforced concrete hollow and ribbed slabs, so that designers can guarantee their fire resistance class when using such structures in construction. This will ensure the safety of mankind during evacuation in the event of a fire in buildings with such constructions by preventing the spread of dangerous fire factors and the spread of the fire itself. In addition, the use of such building structures, taking into account the requirements for ensuring integrity during the normalized time specified in the fire resistance class, will allow emergency and rescue units to effectively and quickly localize the fire.

Each of the methods of the hierarchical system of calculating the fire resistance of reinforced concrete hollow and ribbed slabs according to the onset of the limit state of loss of integrity must have three main aspects: a set of initial data, a calculation algorithm and a method of interpreting the calculation results, i.e. a criterion base indicating the onset or non-occurrence of the limit state of loss integrity



## 3.1 FEATURES OF THE HIERARCHICAL STRUCTURE OF CALCULATION METHODS FOR ASSESSING THE FIRE RESISTANCE OF HOLLOW SLABS BY LOSS OF INTEGRITY

### 3.1.1 IMPROVEMENT OF THE TABULAR CALCULATION METHOD FOR ASSESSING THE FIRE RESISTANCE OF REINFORCED CONCRETE HOLLOW SLABS

According to EN 1992-1-2, *Table 5.9* shows the minimum geometrical dimensions of the slabs required to ensure the corresponding fire resistance class. However, this table is provided for slabs with a thickness of up to 200 mm, which does not make it possible to use it for assessing the fire resistance of hollow slabs with a thickness of 220 mm to 300 mm. Therefore, in order to carry out a simplified assessment of the fire resistance of hollow slabs upon the onset of the limit

state of loss of integrity, it is necessary to supplement the corresponding *Table 5.9* presented in EN 1992-1-2, using the data obtained using the approaches proposed in [5].

For a comprehensive study, it was proposed to follow the regularity of the dependence of the fire resistance limit of reinforced concrete hollow slabs on their most significant geometric parameters, in this case, it is the axial distance of the reinforcing bars and the thickness of the slab.

According to our assumption, the fire resistance limit is related to the geometric parameters of reinforced concrete hollow slabs by a linear polynomial dependence of the type:

$$y = b_0 + b_1 x_1 + b_2 x_2 + b_3 x_1 x_2, \tag{3.1}$$

where $x_1$, $x_2$ – factors that correspond to the initial parameters of reinforced concrete hollow slabs, in our case it is the axial distance of reinforcing bars and slab thickness. This type of regression was chosen based on the results of research given in works [8, 9].

In this case, to establish the regression dependence of this type, the matrix of the experimental plan is used, which has the form of a **Table 3.1**.

In the **Table 3.2**, the intervals of factors for the implementation of a full factorial experiment are given.



**Table 3.1** Planning matrix of a full factorial experiment for building a regression

| No. | $x_1$ | $x_2$ | $x_1x_2$ |
|---|---|---|---|
| 1 | + | + | + |
| 2 | + | – | – |
| 3 | – | + | – |
| 4 | – | – | + |

**Table 3.2** Intervals of variation of factors in a full factorial experiment

| Slab thickness, $H$, mm | | | Axial distance, $w$, mm | | |
|---|---|---|---|---|---|
| Lowest value, $H_{-1}$ | Average value, $H_0$ | Largest value, $H_1$ | Lowest value, $w_{-1}$ | Average value, $w_0$ | Largest value, $w_1$ |
| 220 | 260 | 300 | 10 | 20 | 30 |

To obtain reference data for the implementation of a full factorial experiment, the most common structural characteristics of reinforced concrete hollow slabs were adopted. Mechanical characteristics of concrete and reinforcing steel, as well as geometric characteristics of reinforcement are given in **Table 3.3**.

By varying the relevant parameters according to the matrix of the plan according to the **Table 3.1** and **Table 3.2** according to the results of the calculations according to the proposed

mathematical models of the refined calculation method and using the parameters from the **Table 3.3**, obtained data for conducting a full factorial experiment, which are shown in **Table 3.4**.

**Table 3.3** Technical data for reinforced concrete hollow slab

| Parameter | Units of measurement | Value |
|---|---|---|
| **Concrete** | | |
| Strength class | | C 20/25 |
| Density | kg/m$^3$ | 2400 |
| Strength limit | MPa | 20 |
| Poisson's ratio | | 0.3 |
| The thickness of the concrete between the cavity and the upper slab | mm | 40 mm at $H$=300 mm<br>28 mm at $H$=220 mm |
| **Working armature** | | |
| Strength class | | A400 |
| Strength limit | MPa | 400 |
| Diameter | mm | 12 |
| Applied load as a percentage of the maximum | % | 70 |

**Table 3.4** Parameters of fires in model rooms during a full factorial experiment according to the adopted planning matrix

| Experimental situation | 1 | 2 | 3 | 4 |
|---|---|---|---|---|
| Limit of fire resistance, $U_e$, min | 75 | 51 | 64 | 41 |

When using the results of the full factorial experiment given in **Table 3.4**, the corresponding coefficients of the regression dependence (3.1) were calculated according to the formulas [8, 9]:

$$b_0 = \frac{1}{N}\sum_{i=1}^{N} y_i;\ b_1 = \frac{1}{N}\sum_{i=1}^{N} x_1 y_i;\ b_2 = \frac{1}{N}\sum_{i=1}^{N} x_2 y_i;\ b_3 = \frac{1}{N}\sum_{i=1}^{N} x_1 x_2 y_i. \quad (3.2)$$

where $N$=4 – the number of experimental situations according to the matrix of the full factorial experiment (**Table 3.1**); $x_i$ – values of the corresponding factor according to the matrix of the plan and the ranges of their variation (**Tables 3.1**, **3.2**); $y_i$ – the value of the fire resistance limit according to the results of the corresponding numerical experiments according to the **Table 3.4**.

When applying formulas (3.2), regression coefficients were calculated, which are summarized in the **Table 3.5**.

**Table 3.5** Regression coefficients for determining the limit of fire resistance of reinforced concrete hollow slabs according to the onset of the limit state of loss of integrity

| **Regression coefficients (7.1)** | $b_0$ | $b_1$ | $b_2$ | $b_3$ |
|---|---|---|---|---|
| Encoded values | 57.75 | 5.25 | 11.75 | 0.25 |
| Real values | 3.37 | 0.119 | 1.01 | 0.000625 |

The constructed regression allows to follow the dependence of the fire resistance limit of reinforced concrete hollow slabs on the thickness of the slab and the axial distance of the reinforcing bars. Thus, the revealed regularity of the limit of fire resistance of reinforced concrete hollow slabs upon the onset of the limit state of loss of integrity from the cross-section height ($H$) and the axial distance from the armature to the heating surface of the slab ($w$) can be described with the help of a regression dependence:

$$U_e = 3.37 + 0.119H + 1.01w + 0.000625 \times H \times w. \quad (3.3)$$

It is also possible to present it with the help of the corresponding constructed surface, which is presented in **Fig. 3.1**. It can be seen on the constructed surface that it has an almost exact flat shape.

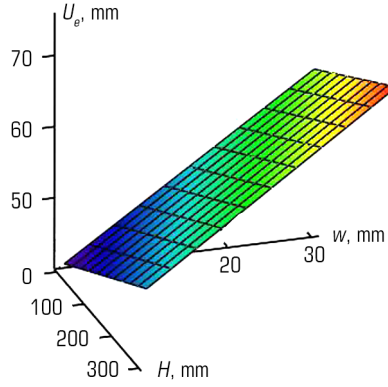


**Fig. 3.1** The surface corresponding to the dependence of the fire resistance limit of a reinforced concrete hollow slab upon the onset of the limit state of loss of integrity on its thickness and the axial distance of the reinforcing bars

It is convenient to determine the limit of fire resistance of reinforced concrete hollow slabs upon the onset of the limit state of loss of integrity according to their most significant structural parameters when using the nomogram presented in **Fig. 3.2**.

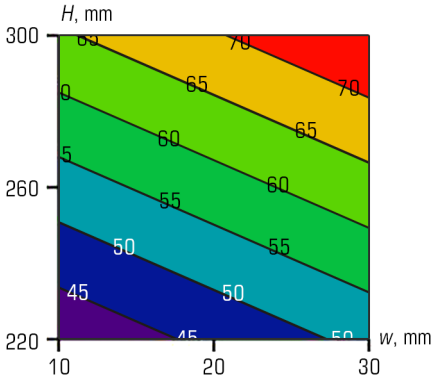


**Fig. 3.2** Nomograms of the dependence of the fire resistance limit of a reinforced concrete hollow slab upon the onset of the limit state of loss of integrity on its thickness and the axial distance of the reinforcing bars

When analyzing the results of the calculated fire resistance assessment based on the onset of the limit state of loss of integrity, the value of the fire resistance limit, determined by the regression dependence and by the refined method, was compared. At the same time, absolute deviation and relative deviation were used as criteria for the adequacy of the calculated results. The data obtained during the analysis of the adequacy of the calculation results according to the regression dependence are presented in the **Table 3.6**.

**Table 3.6** Adequacy of the results of assessing the fire resistance limit of reinforced concrete hollow slabs, determined by regression dependence

| Limit of fire resistance, calculated according to MSE, min | Limit of fire resistance, calculated by regression dependence, min | Absolute deviation, min | Relative deviation, % |
|---|---|---|---|
| Slab thickness $H$=220 mm, Axial distance $w$=15 mm | | | |
| 51 | 46.75 | 4.25 | 8.33 |
| Slab thickness $H$=220 mm, Axial distance $w$=20 mm | | | |
| 60.5 | 52.5 | 8 | 13.223 |
| Slab thickness $H$=300 mm, Axial distance $w$=15 mm | | | |
| 67 | 57 | 10 | 14.925 |
| Slab thickness $H$=300 mm, Axial distance $w$=20 mm | | | |
| 71 | 63 | 8 | 11.268 |
| Average values | | | |
| – | – | 7.563 | 11.937 |

The results of the adequacy analysis are given in **Table 3.6**, indicate that the error of the assessed fire resistance assessment for reinforced concrete hollow slabs, calculated according to the regression dependence, is insignificant and the obtained regression dependence can be used for the assessed fire resistance assessment of reinforced concrete hollow slabs according to the limit state of loss of integrity.

When using the nomogram shown in **Fig. 3.2**, the *Table 5.9*, given in the guideline EN 1992-1-2, was clarified. The updated table is presented in the form of a **Table 3.7**.

**Table 3.7** Minimum dimensions and axial distances for reinforced concrete hollow slabs

| Standard fire resistance | Minimum dimensions (mm) | |
|---|---|---|
| | Slab thickness, $h_s$ | Axial distance, $a$ |
| REI 30 | 220 | 15 |
| REI 45 | 220 | 20 |
| REI 60 | 220/300 | 30/20 |
| REI 90 | 300 | 35 |



The implementation of the refined tabular method of assessing the fire resistance of reinforced concrete hollow slabs by the onset of the limit state of loss of integrity has the simplest algorithm. Three main parameters are used as initial data: $h_s$ – slab thickness; $a$ – the axial distance of the reinforcing bars to the heating surface; REI – fire resistance class that must be provided.

To implement the algorithm of the tabular method, a **Table 3.6** is used. For the required class of fire resistance, the appropriate line is selected, which contains the minimum values of the slab thickness and the axial distance of the reinforcing bars. If the real parameters are greater, then the required fire resistance class is considered to be provided.

### 3.1.2 DEVELOPMENT OF A SIMPLIFIED METHOD FOR ASSESSING FIRE RESISTANCE BY LOSS OF INTEGRITY FOR HOLLOW SLABS

To implement the algorithm of the simplified method of calculating the fire resistance of reinforced concrete hollow slabs upon the onset of the limit state of loss of integrity with the use of mathematical models of crack formation, described in [5, 10], a set of initial data is used, which is given in **Table 3.8**.

When calculating according to a mathematical model, a strength criterion was developed, which can be written through the expression:

$$f_{ct,\theta}^2 + \sigma_y f_{ct,\theta} - \tau_{xy}^2 = 0. \quad (3.4)$$

The voltages in equation (3.4) are calculated according to the formulas:

$$\sigma_y = \frac{F_p \operatorname{tg}\varphi_c}{b_s h_p}, \tau_{xy} = \frac{F_p}{b_s h_p}, \quad (3.5)$$

where $b_s$ – the slab width.

By substituting these values into equation (3.4) and solving it with respect to the limit force $F_p$, the possibility of crack formation was analyzed according to the mechanism reproduced in the diagram of **Fig. 3.3**.

**Table 3.8** A set of initial data for the implementation of a simplified method of assessing the fire resistance of reinforced concrete hollow slabs according to the limit state of loss of integrity

| **Materials data** | | | | |
|---|---|---|---|---|
| Concrete strength class | Reinforcement strength class | The law of concrete deformation | The law of reinforcement deformation | The law of change of temperature deformation |
| **Data on design parameters** | | | | |
| Slab dimensions | The geometry of the armature location | Diameters and number of reinforcing bars | | |
| Data on the temperature distribution in the cross section | | | | |
| Nomogram of temperature distribution | | | | |

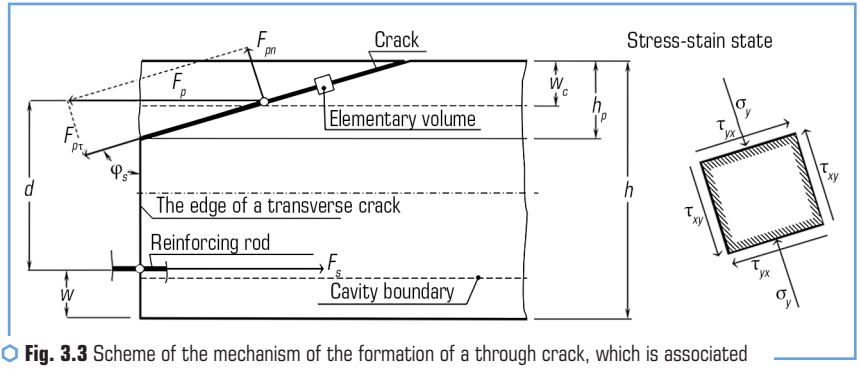


**Fig. 3.3** Scheme of the mechanism of the formation of a through crack, which is associated with the onset of the limit state of loss of integrity

When analyzing all possible solutions of equation (3.4), there are no real roots. Therefore, another mechanism operates during the formation of cracks, which is shown in the diagram of **Fig. 3.4**.

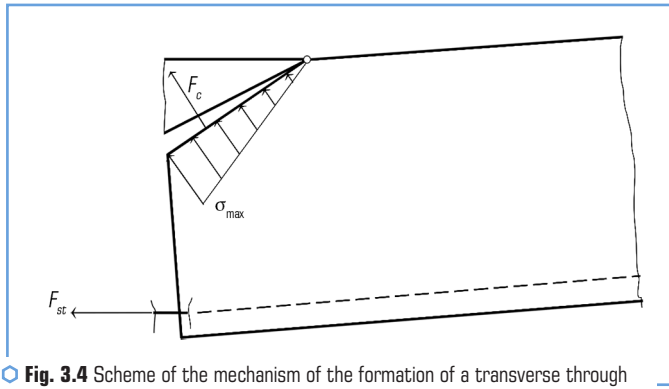


**Fig. 3.4** Scheme of the mechanism of the formation of a transverse through crack, which is associated with the onset of the limit state of loss of integrity

According to the calculation scheme shown in **Fig. 3.4**, the equilibrium equation was compiled:

$$F_{st}\left(h-w_c\right)+\frac{2}{3}\frac{F_c h_p}{\sin\varphi_c}=M_E, \tag{3.6}$$

where $M_E$ – the acting moment from the distributed load applied to the slab.

The force in the reinforcing bar and the force of detachment of the lateral surface of the prism of the destruction of a reinforced concrete hollow slab are determined, respectively, by the formulas:

$$F_{st}=f_{s,\theta}\frac{\pi\cdot d_s^2}{4};\ F_c=\frac{f_{ct,\theta}h_p b_s}{2\sin\varphi_c}. \tag{3.7}$$

In view of the given expressions, the distance from the upper surface of the slab to the starting point of the formation of a through crack can be determined by the formula:

$$h_p=\sqrt{\frac{3\sin^2\varphi_A}{f_{ct,\theta}b_s}\left(\frac{q_E l^2}{8}-f_{s,\theta}\frac{\pi\cdot d_s^2}{4}\right)}\le w_c. \tag{3.8}$$

Thus, using this formula, it is possible to determine the danger of the formation of a through crack. The condition for the formation of a through crack is dangerous if the distance $h_p$ exceeds the distance from the upper surface of the slab to the cavity rib $w_c$.

Another possible prerequisite for the occurrence of the limit state of loss of integrity can be the formation of longitudinal through cracks between the upper rib of the cavity and the upper surface of the slab. The mechanism of formation of this type of cracks can be illustrated by the diagram shown in **Fig. 3.5**.

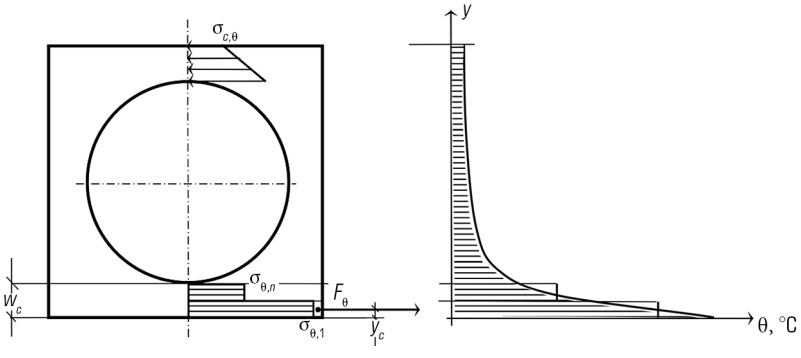


**Fig. 3.5** Scheme of the mechanism of the formation of a transverse through crack, which is associated with the onset of the limit state of loss of integrity

Considering the calculation scheme shown in **Fig. 3.5**, it is possible to write the equilibrium equation describing the stress-strain state in the corresponding inner layers of the reinforced concrete slab:

$$\sigma_{c,\theta} = \frac{F_\theta}{w_c l}\left[1 - 6w_c^{-1}\left(h - 0.5w_c - y_c\right)\right]. \tag{3.9}$$

Here, the force acting as a result of thermal expansion in the lower layers of a fragment of a reinforced concrete slab is determined by the formula:

$$F_\theta = \frac{1}{n} w_c l \sum_{i=1}^{n} \sigma_{\theta i}\left(\varepsilon_c(\theta)\right). \tag{3.10}$$

Equation (3.9) also includes the distance from the bottom surface of the slab to the point of application of the force $F_\theta$, which is determined by the formula:

$$y_c = \frac{\sum_{i=1}^{n} y_i \sigma_{\theta i}\left(\varepsilon_c(\theta)\right)}{\sum_{i=1}^{n} \sigma_{\theta i}\left(\varepsilon_c(\theta)\right)}. \tag{3.11}$$

Stresses arising as a result of temperature deformations are determined by the formulas given in the first column of the *Table 1*, given in [1]. As deformations, a mathematical model of the dependence of temperature deformations on temperature is used here, which is described by the following expressions:

$$\varepsilon_c(\theta) = -1.8 \cdot 10^{-4} + 9 \cdot 10^{-6}\theta + 2.3 \cdot 10^{-11}\theta^3 \text{ at } 20\ ^\circ\text{C} \le \theta \le 70\ ^\circ\text{C};$$
$$\varepsilon_c(\theta) = 14 \cdot 10^{-3} \text{ at } 700\ ^\circ\text{C} \le \theta \le 1200\ ^\circ\text{C}. \tag{3.12}$$

The resulting calculation methods allow analyzing the conditions of crack formation, which can be considered as signs of the onset of the limit state of loss of fire resistance in terms of integrity. The proposed methods have a hierarchical structure at the base of which are simplified methods, while at the top the refined methods proposed by us are based on the finite element method.

When performing the calculation according to the mathematical model (3.6–3.8), it is necessary to determine the temperature distribution over the thickness of the slab, for this, a diagram (**Fig. 3.6**) is used, which is recommended by the guidelines in the EN 1992-1-2 standard. With its use, it is possible to determine the temperature of the reinforcing bars and the heating temperature of the inner layers of the concrete slab.

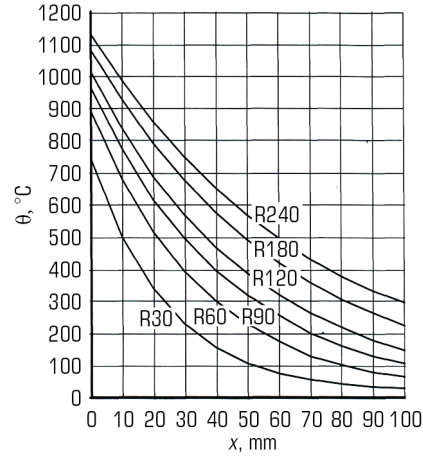


**Fig. 3.6** Nomogram for determining the temperature distribution in a reinforced concrete hollow slab

The reduced strength of reinforcing steel is determined by the formula:

$$f_{s,q} = k_t(\theta) f_s, \tag{3.13}$$

where $k_t(\theta)$ – the coefficient of reduction of the tensile strength of reinforcing steel.

The average reduced strength of the reinforcement row depending on the elevated temperatures according to the EN 1992-1-2 guideline is calculated by the formula:

$$k_v(\theta) = \frac{\sum k_t(\theta_i)}{n_v}, \tag{3.14}$$

where $k(\theta_i)$ – the strength reduction factor of the $i$-th reinforcing bar depending on the temperature $\theta_i$ obtained from the nomogram in **Fig. 3.6**; $k_v(\theta)$ – the average strength reduction factor of the $v$-th reinforcement row; $n_v$ – the number of reinforcing bars in the $v$-th reinforcing row.

The distance a from the lower surface of the calculated cross-section to the center of gravity of the reinforcement row can be calculated by the formula:

$$a = \frac{\sum a_v k_v(\theta)}{\sum k_v(\theta)}, \tag{3.15}$$

where $a_v$ – the distance from the lower surface of the calculated cross-section to the $v$-th reinforcement row.

If there are only two rows, the distance $w$ from the lower surface of the calculated cross-section to the center of gravity of the reinforcing row can be calculated using the following formula:

$$w = \sqrt{(a_1 a_2)}. \tag{3.16}$$

If the reinforcing bars have different areas and are placed arbitrarily, the following technique is used.

The average resistance of the reinforcing steel group $k(\varphi)f_{s,fi}$ depending on the elevated temperatures can be calculated by the expression:

$$k(\varphi)f_{sd,fi} = \frac{\sum_i \left[k_s(\theta_i) f_{s,i} A_i\right]}{\sum_i A_i}, \tag{3.17}$$

where $k_t(\theta_i)$ – the strength reduction factor of the $i$-th reinforcing bar; $f_{s,i}$ – calculated resistance of the $i$-th reinforcing bar; $A_i$ – cross-sectional area of the $i$-th reinforcing bar.

The distance w from the calculated cross-section to the center of gravity of the reinforcement group is calculated according to the formula (3.18):

$$w = \frac{\sum_i \left[a_i k_s(\theta_i) f_{s,i} A_i\right]}{\sum_i \left[k_s(\theta_i) f_{s,i} A_i\right]}, \tag{3.18}$$

where $a_i$ – the distance from the calculated cross-section to the axis of the $i$-th reinforcing bar.

The average coefficient of reduction of concrete strength for the section of the element is determined by the zone method, including the coefficient $(1–0.2/n)$, which takes into account the temperature change of each zone in the calculation according to the formula:

$$k_c = \frac{(1-0.2/n)}{n} \sum_{i=1}^{n} k_{c,i}(\theta_i), \tag{3.19}$$

where $n$ – the number of zones (minimum $n=3$, recommended $n=5$).

The reduced strength of concrete in the compressed zone of the slab is determined by the formula:

$$f_{ct,q} = k_c(\theta) f_{ct}. \quad (3.20)$$

In this way, the implementation of the proposed method can be carried out according to the algorithm, the scheme of which is presented in **Fig. 3.7**.

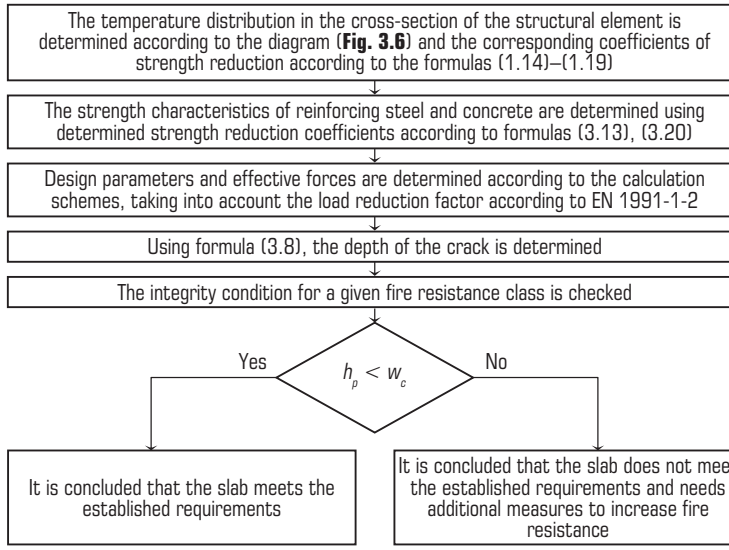


**Fig. 3.7** Scheme of the algorithm for the implementation of the method for calculating the fire resistance of a reinforced concrete hollow slab based on the limit state of the loss of integrity when transverse cracks appear

To carry out the calculation according to this method, a set of initial data is also required, which is presented in the form of the **Table 3.8**.

When implementing the algorithm for calculating integrity based on the occurrence of longitudinal cracks, the scheme in **Fig. 3.8** can be used.

Both of the described methods must be applied in a complex and if one of them gives a negative result, it is considered that the slab does not meet the established requirements for fire resistance according to the limit state of loss of integrity.

The next step in the hierarchy of methods for calculating the fire resistance of a reinforced concrete hollow slab based on the limit state of loss of integrity requires the use of refined methods. In [5, 10] it is shown that these methods allow, based on the calculation results, to identify the

moment of onset of the limit state of loss of integrity. To carry out the calculation according to this method, a set of initial data is also required, which is presented in the form of a **Table 3.8**. Basic mathematical models and theoretical references given in the **Table 3.9** are also used for conducting.

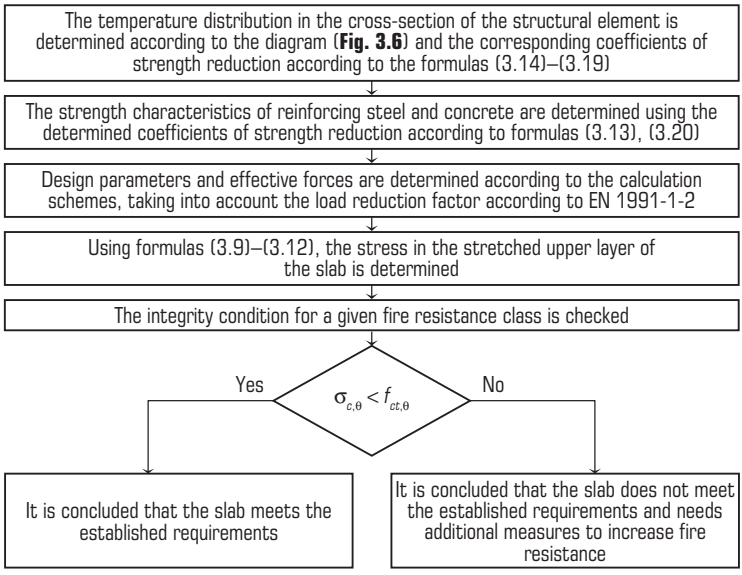


**Fig. 3.8** Scheme of the algorithm for the implementation of the method for calculating the fire resistance of a reinforced concrete hollow slab based on the limit state of the loss of integrity when longitudinal cracks appear

**Table 3.9** Basic methods of numerical investigation of the integrity of reinforced concrete hollow slabs in case of fire

| **Component of a mathematical model** | **Used calculation methods** |
|---|---|
| **1** | **2** |
| **Heat engineering problem** | |
| Thermal conductivity | Differential non-stationary heat conduction equation, approximated by the finite element method [11] |
| Boundary conditions | Boundary conditions of the III kind, taking into account convection and radiant heat exchange [11] |
| Physical nonlinearity | Newton-Raphson method [12] |
| Thermophysical characteristics | Recommended by EN 1992-1-2 |
| Characteristics of boundary conditions | Recommended by EN 1992-1-2 |

**Continuation of the Table 3.9**

| 1 | 2 |
|---|---|
| **Structural task** | |
| Stressed and deformed state | Finite element method in nonlinear implementation [12] |
| Plastic deformation | Associative theory of plasticity [12] |
| Crack formation criterion | Willem-Warnke concrete strength criterion [12] |
| Physical and geometric nonlinearity | Newton-Raphson method [12] |
| Mechanical and thermomechanical characteristics | Deformation diagrams recommended by EN 1992-1-2 |
| Software tools | ANSYS Workbench, ANSYS APDL Mechanical, ABAQUS |

When using the method next in the hierarchy, the algorithm for integrating the equations of mechanics by the implicit method is used. This algorithm can be implemented using the scheme presented in **Fig. 3.9**.

At the top of the hierarchical system of methods for calculating the fire resistance of a reinforced concrete hollow slab according to the limit state of the loss of integrity in the scheme of **Fig. 3.10** is a method using explicit integration of the dynamics equations.



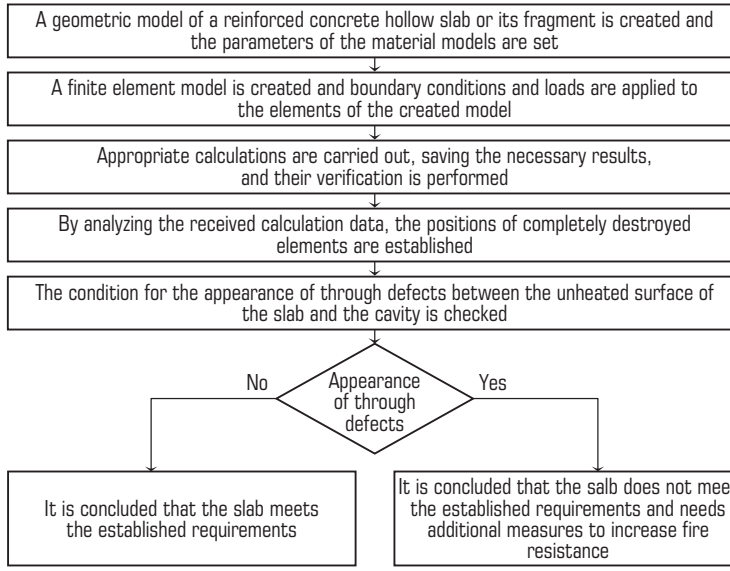


**Fig. 3.9** Scheme of the algorithm for the implementation of the refined method of fire resistance with implicit integration for a reinforced concrete hollow slab under the limit state of loss of integrity with the appearance of transverse cracks

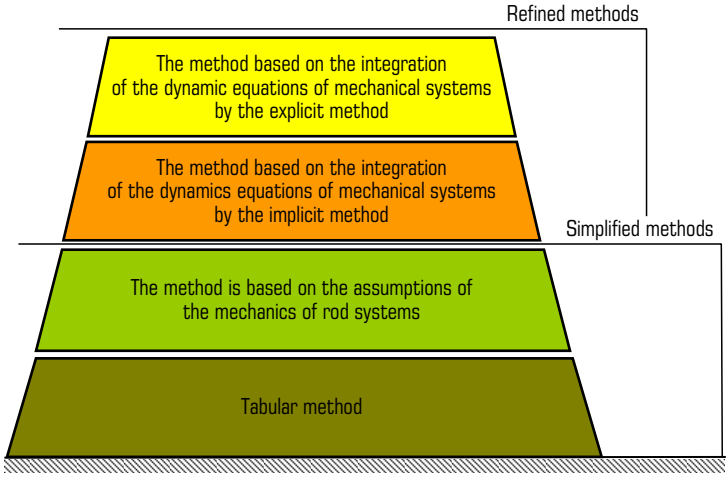


**Fig. 3.10** Hierarchical system of methods for assessing the fire resistance of reinforced concrete hollow and ribbed slabs according to the onset of the limit state of loss of integrity

In [10] it is shown that this method also allows to identify the moment of onset of the limit state of loss of integrity based on the calculation results. To carry out the calculation according to this method, a set of initial data is also required, which is presented in the form of a **Table 3.8**, the main mathematical models and theoretical references given in the **Table 3.9** are also used for the implementation.

According to the **Table 3.10** to implement this method, there must be specialized software.

**Table 3.10** Basic methods of numerical investigation of the integrity of reinforced concrete hollow slabs in case of fire

| **Component of a mathematical model** | **Used calculation methods** |
|---|---|
| **1** | **2** |
| **Heat engineering problem** | |
| Thermal conductivity | Differential non-stationary heat conduction equation, approximated by the finite element method [1] |
| Boundary conditions | Boundary conditions of the III kind, taking into account convection and radiant heat exchange [11] |
| Physical nonlinearity | Newton-Raphson method [12] |
| Thermophysical characteristics | Recommended by EN 1992-1-2 |
| Characteristics of boundary conditions | Recommended by EN 1992-1-2 |

**Continuation of the Table 3.10**

| 1 | 2 |
|---|---|
| **Structural task** | |
| Stressed and deformed state | Finite element method in nonlinear implementation with explicit integration of dynamics equations [13] |
| Plastic deformation | Associative theory of plasticity [14] |
| Crack formation criterion | Concrete model CSCM (Continuous Surface Cap Model) [15] |
| Physical and geometric nonlinearity | Newton-Raphson method [12] |
| Mechanical and thermomechanical characteristics | Deformation diagrams recommended by EN 1992-1-2 |
| Software tools | ANSYS LS-DYNA |

When using this method, the next in the hierarchy, the algorithm for integrating the equations of mechanics according to the explicit method is used. At the same time, the dynamics equations are integrated in the general formulation. This method allows to avoid difficulties with the convergence of processes. Also, this method makes it possible to obtain direct signs of the onset of the limit state of loss of integrity.

The described algorithm can also be implemented using the circuit shown in **Fig. 3.9**.



## 3.2 FEATURES OF THE HIERARCHICAL STRUCTURE OF CALCULATION METHODS FOR ASSESSING THE FIRE RESISTANCE OF RIBBED SLABS BY LOSS OF INTEGRITY

### 3.2.1 IMPROVEMENT OF THE TABULAR CALCULATION METHOD FOR ASSESSING THE FIRE RESISTANCE OF REINFORCED CONCRETE RIBBED SLABS

In EN 1992-1-2, as well as for hollow slabs, a similar *Table 5.10* is given for ribbed slabs about certain minimum geometric dimensions of these slabs to ensure the corresponding class of fire resistance. However, this table may be refined in light of new integrity loss data obtained using the approaches proposed in [7]. For a comprehensive study, it was proposed to follow the regularity of the dependence of the fire resistance limit of reinforced concrete ribbed slabs on their most significant geometric parameters, in this case, it is the axial distance of the reinforcing bars and the thickness of the panel in the cell between the ribs of the slab.

According to the accepted assumption, the limit of fire resistance of ribbed slabs is related to the geometric parameters of these structures by a polynomial dependence, just like hollow slabs [8, 9].

In this case, to establish the regression dependence of this type, the matrix of the experimental plan is used, which has the form of a **Table 3.1**.

The **Table 3.11** shows the intervals of factors for the implementation of a full factorial experiment.

**Table 3.11** Intervals of variation of factors in a full factorial experiment

| **The thickness of the panel in the cell between the slab ribs, *H*, mm** | | | **The axial distance of the reinforcing bars to the heating surface of the panel between the slab ribs, *w*, mm** | | |
|---|---|---|---|---|---|
| **Lowest alue, $H_{-1}$** | **Average value, $H_0$** | **Largest value, $H_1$** | **Lowest value, $w_{-1}$** | **Average value, $w_0$** | **Largest value, $w_1$** |
| 30 | 55 | 80 | 10 | 15 | 20 |

To obtain reference data for the implementation of a full factorial experiment, the most common structural characteristics of reinforced concrete ribbed slabs were adopted. Mechanical characteristics of concrete and reinforcing steel, as well as geometric characteristics of reinforcement are given in **Table 3.12**.

**Table 3.12** Technical data on reinforced concrete ribbed slab

| **Parameter** | **Units of measurement** | **Value** |
|---|---|---|
| **Concrete** | | |
| Strength class | | C 20/25 |
| Density | kg/m$^3$ | 2400 |
| Strength limit | MPa | 20 |
| Poisson's ratio | | 0.3 |
| The height of the longitudinal ribs | mm | $H_m$=300 mm |
| The height of the transverse ribs | mm | $H_a$=140 mm |
| **Working reinforcement in longitudinal ribs** | | |
| Strength class | | A400 |
| Strength limit | MPa | 400 |
| Diameter | mm | 16 |
| **Working fittings in transverse ribs** | | |
| Strength class | | A400 |
| Strength limit | MPa | 400 |
| Diameter | mm | 12 |
| **Working fittings in the panel between the ribs** | | |
| Strength class | | A400 |
| Strength limit | MPa | 400 |
| Diameter | mm | 8 |
| Applied load on the slab | | |
| Applied load as a percentage of the maximum | % | 70 |

By varying the relevant parameters according to the matrix of the plan according to the **Table 3.1** and **Table 3.12** according to the results of the calculations [6, 7] according to the proposed mathematical models of the refined calculation, obtained data for conducting a full factorial experiment, which are shown in **Table 3.13**.

When using the results of the full factorial experiment given in **Table 3.13**, the corresponding coefficients of the regression dependence (3.1) were calculated according to the formulas (3.2) [8, 9].

When applying formulas (3.2), regression coefficients were calculated, which are summarized in the **Table 3.14**.

**Table 3.13** Parameters of fires in model rooms during a full factorial experiment according to the adopted planning matrix

| **Experimental situation** | **1** | **2** | **3** | **4** |
|---|---|---|---|---|
| Limit of fire resistance, $U_e$, min | 46 | 26 | 33 | 18 |

**Table 3.14** Regression coefficients for determining the limit of fire resistance of reinforced concrete hollow slabs by the onset of the limit state of loss of integrity

| **Regression coefficients (7.1)** | $b_0$ | $b_1$ | $b_2$ | $b_3$ |
|---|---|---|---|---|
| Encoded values | 30.75 | 5.25 | 8.75 | 1.25 |
| Real values | 1.2 | 0.06 | 1.2 | 0.01 |



The constructed regression allows to follow the dependence of the fire resistance limit of reinforced concrete ribbed slabs on the panel thickness in the cells between the ribs and the axial distance of the reinforcing rods in this panel.

Thus, the revealed regularity of the limit of fire resistance of reinforced concrete ribbed slabs according to the loss of integrity from the cross-sectional thickness of the panel between the ribs ($h_s$) and the axial distance from the reinforcement to the heating surface of the panel between the ribs ($w_s$) can be described using a regression relationship:

$$U_e = 1.2 + 0.06h_s + 1.2w_s + 0.01 \times h_s \times w_s. \quad (3.21)$$

Also, the detected regularity can be presented using the corresponding constructed surface, which is presented in **Fig. 3.11**. It can be seen on the constructed surface that it has an almost exact flat shape.

It is convenient to determine the limit of fire resistance of reinforced concrete ribbed slabs according to their most significant structural parameters when using the nomogram presented in **Fig. 3.12**.

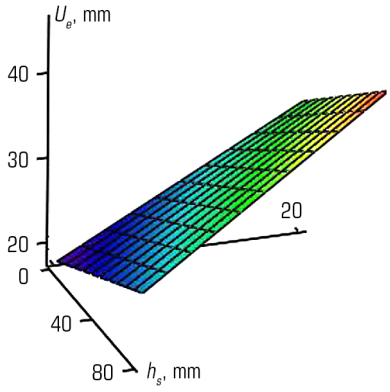


**Fig. 3.11** The surface corresponding to the dependence of the fire resistance limit of a reinforced concrete ribbed slab upon the onset of the limit state of loss of integrity on the slab thickness in the cells between the ribs and the axial distance of the reinforcing rods in the panel

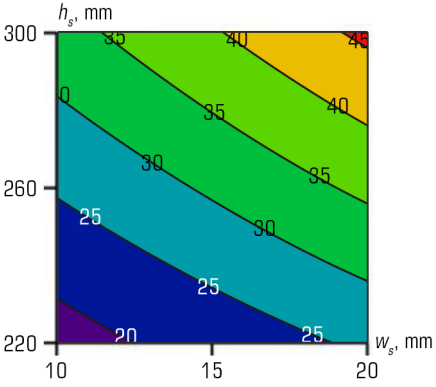


**Fig. 3.12** Nomograms of the dependence of the fire resistance limit of a reinforced concrete ribbed slab upon the onset of the limit state of loss of integrity on the slab thickness in the cells between the ribs and the axial distance of the reinforcing rods in the panel

When analyzing the results of the calculated assessment of fire resistance upon the onset of the limit state of loss of integrity, the value of the fire resistance limit, determined by regression dependence and by the refined method, was compared. At the same time, absolute deviation and

relative deviation were used as criteria for the adequacy of the calculated results. The data obtained during the analysis of the adequacy of the calculation results according to the regression dependence are presented in the **Table 3.15**.

**Table 3.15** Adequacy of the results of assessing the fire resistance limit of reinforced concrete ribbed slabs, determined by regression dependence

| Limit of fire resistance, calculated according to MSE, min | Limit of fire resistance, calculated by regression dependence, min | Absolute deviation, min | Relative deviation, % |
|---|---|---|---|
| Slab thickness between the ribs $h_s$=30 mm, Axial distance $w_s$=15 mm | | | |
| 27.1 | 25.5 | 1.6 | 5.904 |
| Slab thickness $H$=50 mm, Axial distance $w$=15 mm | | | |
| 32 | 29.7 | 2.3 | 7.188 |
| Slab thickness $H$=80 mm, Axial distance $w$=15 mm | | | |
| 44 | 38 | 6 | 13.634 |
| Slab thickness $H$=80 mm, Axial distance $w$=20 mm | | | |
| 48 | 46 | 2 | 4.167 |
| Average values | | | |
| – | – | 2.975 | 7.724 |

The results of the adequacy analysis are given in **Table 3.15**, indicate that the error of the assessed fire resistance for reinforced concrete ribbed slabs, calculated according to the regression dependence, is insignificant and the obtained regression dependence can be used for the assessed fire resistance of reinforced concrete hollow slabs according to the limit state of loss of integrity.

When using the nomogram shown in **Fig. 3.12**, a part of the *Table 5.10* EN 1992-1-2 was clarified. The detailed part of the table is presented below in the form of a **Table 3.16**.

**Table 3.16** Minimum dimensions and axial distances for reinforced concrete ribbed slabs

| Standard fire resistance | Minimum dimensions (mm) | | | | |
|---|---|---|---|---|---|
| | Possible combinations of rib width $b_{min}$ and axial distance $a$ | | | Thickness $h_s$ and axial distance $w_s$ in the slab shelf | |
| REI 15 | $b_{min}$=80<br>$a$=15 | | | $h_s$=30<br>$w_s$=15 | $h_s$=50<br>$w_s$=10 |
| REI 30 | $b_{min}$=80<br>$a$=15 | | | $h_s$=50<br>$w_s$=15 | |
| REI 45 | $b_{min}$=80<br>$a$=15 | | | $h_s$=50<br>$w_s$=25 | |
| REI 60 | $b_{min}$=100<br>$a$=35 | 120<br>25 | ≥200<br>15* | $h_s$=80<br>$w_s$=10* | |

The implementation of the tabular method of assessing the fire resistance of reinforced concrete ribbed slabs by the onset of the limit state of loss of integrity has the simplest algorithm. Three main parameters are used as initial data: $b_{min}$ – slab rib thickness; $a$ – axial distance of reinforcing bars of the rib to the heating surface; $h_s$ – the thickness of the slab panel between the ribs of the slab; $w_s$ – the axial distance of the reinforcing bars of the panel to the heating surface; REI – the fire resistance class that must be provided.

**Table 3.16** is used to implement the algorithm of the tabular method. For the required class of fire resistance, the appropriate line is selected, which contains the minimum values of the thickness of the slab shelf and the axial distance of the reinforcing bars. If the real parameters are greater, then the required fire resistance class is considered to be provided.

### 3.2.2 HIERARCHICAL STRUCTURE OF METHODS FOR ASSESSING THE FIRE RESISTANCE OF REINFORCED CONCRETE RIBBED SLABS ACCORDING TO THE ONSET OF THE LIMIT STATE OF LOSS OF INTEGRITY

The conducted studies, the results of which are described in [7], make it possible to form a hierarchical approach to the methods of calculating the fire resistance of reinforced concrete ribbed slabs upon the onset of the limit state of loss of integrity.

The main tool for achieving such a result is the proposed models of crack formation, which have a through character. In general, the data of the model, obtained as a result of the generalization of a large amount of experimental and computational-theoretical data, are used to justify simplified methods.

According to EN 1992-1-2, the hierarchical system of calculation methods for the loss of load-bearing capacity is a structure based on simplified methods and on top of refined methods. The same system is proposed to be used to assess fire resistance at the limit state of loss of integrity for ribbed and hollow slabs. **Fig. 3.10** presents a hierarchical system of methods for calculating reinforced concrete hollow and ribbed slabs according to the limit state of loss of integrity.

### 3.2.3 DEVELOPMENT OF A SIMPLIFIED METHOD FOR CALCULATING THE FIRE RESISTANCE OF REINFORCED CONCRETE RIBBED SLABS ACCORDING TO THE LIMIT STATE OF LOSS OF INTEGRITY

To implement the algorithm of the simplified method of calculating the fire resistance of reinforced concrete ribbed slabs upon the onset of the limit state of loss of integrity, the set of initial data presented in **Table 3.8** is used as for hollow slabs. At the same time, other mathematical models of crack formation are used.

According to the results obtained in the studies on modeling the stress-strain state in reinforced concrete ribbed slabs [7], it is possible to describe the main mechanism of the formation of

defects associated with the onset of the limit state of loss of integrity. According to the obtained data, the loss of integrity occurs when the panel is destroyed between the slab ribs. The whole process of deformation and destruction of the slab takes place in several stages. At the first stage, the slab is deformed under the influence of the active load in the form of its downward bending [7]. After the start of the thermal effect of the standard temperature regime of the fire due to the thermal expansion of the concrete of the panel between the ribs, the bend begins to gradually decrease and at a certain point in time the slab bends upwards, however, under the influence of heating, cells are formed between the ribs, in which the panel bends downwards and acquires the shape of holes [7]. The destruction of the formed cells of the panel between the ribs of the slab at the same time occurs by the formation of cracks along the borders of these cells.

In order to study the mechanism of destruction during the research carried out in [7], distributions of the magnitude of vertical displacements were constructed for reinforced concrete ribbed slabs at different levels of the applied effective load. The constructed distributions are shown in **Fig. 3.13**.

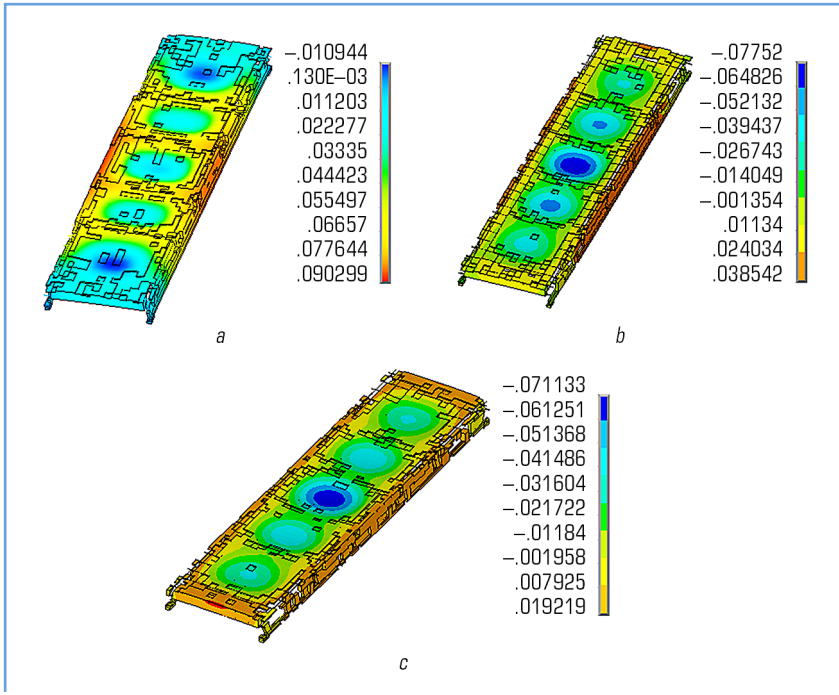


**Fig. 3.13** Distribution of vertical movements (*m*) in the studied reinforced concrete ribbed slab at the time of failure at different levels of the applied active load: *a* – 30 % of the maximum load; *b* – 50 % of the maximum load; *c* – 70 % of the maximum load

It is possible to see in **Fig. 3.13** that the nature of the destruction of the panel between the ribs of a reinforced concrete ribbed slab corresponds to the nature of destruction during fire tests of such slabs, described in [16]. **Fig. 3.14** shows a picture of the destruction of reinforced concrete ribbed slabs.

*a* *b*

**Fig. 3.14** The nature of the destruction of the panel of the ribbed reinforced concrete slab during its fire tests: *a* – during the fire tests; *b* – after the fire tests
*Source: [16]*

The research conducted in [7] showed a high accuracy of reproduction of the processes occurring in reinforced concrete ribbed slabs, and the possibility of using such an approach [7] as a refined method for assessing the fire resistance of reinforced concrete ribbed slabs according to the limit state of loss of integrity.

Therefore, the partial destruction of the ribbed panel by such a mechanism causes the loss of the integrity of this slab.

In general, the above-described mechanism can be illustrated by a geometric diagram that establishes the main features of the formation of defects (**Fig. 3.15**).

In view of the obtained data on the mechanism of destruction of panels between the ribs of a reinforced concrete ribbed slab, the main prerequisites, hypotheses and assumptions were formulated for the creation of a simplified method for calculating fire resistance at the onset of the limit state of loss of integrity, which are as follows:

1. When breaking, the panel in the cell between the ribs of the reinforced concrete ribbed slab breaks along the lines where the "plastic hinges" are located, of two types: the line delineating the outer contour of the fracture zone and straight lines delineating four facets together with the contour line. These facets make up a geometrically variable system.

2. Calculation of the virtual work of external and internal forces is used for the calculation assessment when applying the principle of possible displacements.

3. The criterion for the destruction of a panel between the ribs of a reinforced concrete ribbed slab is the excess of the total virtual work of external forces over the total virtual work of internal forces.

4. The total work of internal forces is determined using the internal limit moments, which are determined using the recommendations of EN 1992-1-2, taking into account the reduction in the resistance of reinforced concrete according to the zone method.

5. Virtual works are calculated on the possible movements of the kinematic system, which is formed on the lines of "plastic hinges".

6. Taking into account the results of research given in works [17, 18], the contour line of the destruction zone is approximated using Bezier lines.

Using the formulated provisions and the scheme presented in **Fig. 3.15**, the calculation scheme presented in **Fig. 3.16** is built.

The line of the outer contour of the panel failure zone in the cell between the ribs of the reinforced concrete ribbed slab can be approximated using the Bezier curve [17, 18]. The use of this type of approximation is determined by the special properties of Bezier curves. The specified curves are continuous according to the first and second order derivatives, allow to take into account the features of the panel failure zone in the cell between the slab ribs with the calculation of the current values of the geometric characteristics for the calculation of both internal and external moments.



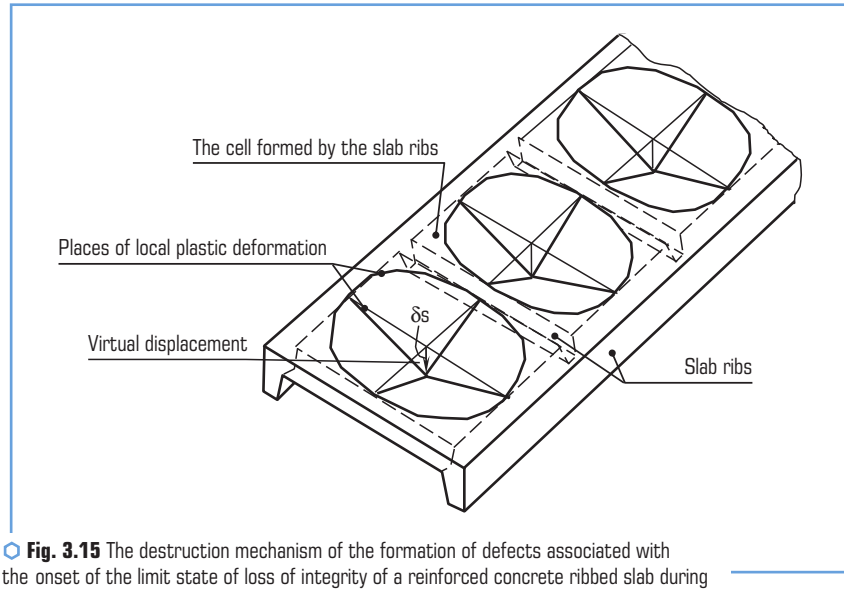


**Fig. 3.15** The destruction mechanism of the formation of defects associated with the onset of the limit state of loss of integrity of a reinforced concrete ribbed slab during exposure to the standard fire temperature regime

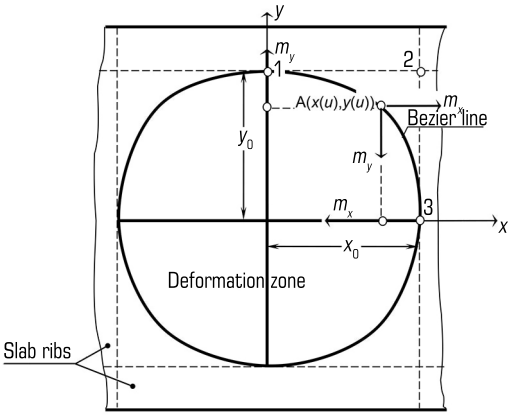


**Fig. 3.16** The calculation scheme for the approximation of the lines of plastic hinges, along which the slab destruction in the cell between the ribs of a reinforced concrete ribbed slab occurs

An additional justification for the fact that Bezier lines best reproduce the line of distribution of "plastic joints" in the slab is the geometric representation of the algorithm for their construction, presented in **Fig. 3.17** [19].

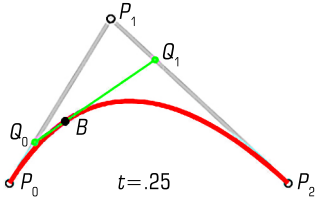


**Fig. 3.17** Geometric scheme of the algorithm for constructing Bezier lines

In **Fig. 3.17** it can be seen that the effective internal plastic moment is directed along the tangent to the curve, which is built on straight lines that limit the zone of destruction in the cell between the slab ribs.

The vector of coordinates of the reference points, through which the form of the Bezier line function is determined, in the general case is calculated by the expression [20]:

$$F(u) = \sum_{k=1}^{n} q_k B_{k,n}(u),\ 0 \le u \le 1, \tag{3.32}$$

where $n=3$ – the number of reference points; $B_{k,n}(u)$ – Bernstein polynomials for matching Bezier lines; $q_k$ – vector of coordinates of reference points for constructing a Bezier line.

Bernstein polynomials are described by the formula:

$$B_{k,n}(u)=\frac{n!}{k!(n-k)!}u^k(1-u)^{n-k}. \tag{3.23}$$

In this case, the vector expression (3.22) is decomposed into an algebraic system consisting of two parametric equations:

$$x(u)=\sum_{k=1}^{n}x_kB_{k,n}(u),\ y(u)=\sum_{k=1}^{n}y_kB_{k,n}(u). \tag{3.24}$$

To formulate the expression for calculating the virtual work of internal forces, the calculation scheme presented in **Fig. 3.18**.

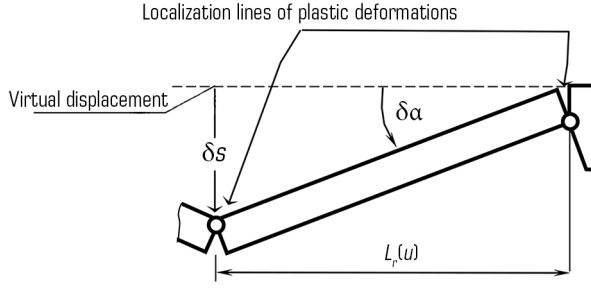


**Fig. 3.18** Scheme for determining possible movements when determining the work of internal forces in the panel failure zone in the cell between the ribs of a reinforced concrete ribbed slab

Considering the schemes presented in **Fig. 3.16**, **3.18**, the elementary work of internal forces for one symmetric quarter of the facet system at a certain point $A(x(u), y(u))$ in orthogonal directions is determined by the expressions:

$$dW_x=\frac{m_x}{L_{rx}(u)}dl(u)+\frac{m_x}{L_{rx}(u)}x_0,\ dW_y=\frac{m_y}{L_{ry}(u)}dl(u)+\frac{m_y}{L_{ry}(u)}y_0. \tag{3.25}$$

Here, the elementary section of the curve and the length on the scheme of the elementary kinematic system (**Fig. 3.17**) are determined by the formulas:

$$dl(u)=\sqrt{\left(\frac{dx(u)}{du}\right)^2+\left(\frac{dy(u)}{du}\right)^2},\ L_{rx}(u)=C(u),\ L_{ry}(u)=x(u). \tag{3.26}$$

Given formulas (3.25) and (3.26), the formula for determining the virtual work of the internal forces of a symmetrical quarter of a mechanical system consisting of facets (**Fig. 3.16**).

$$W=W_x+W_y,$$

$$W_x=m_x\int_0^1\frac{1}{y(u)}\left(\sqrt{\left(\frac{dx(u)}{du}\right)^2+\left(\frac{dy(u)}{du}\right)^2}+x_0\right)du,$$

$$W_y=m_y\int_0^1\frac{1}{x(u)}\left(\sqrt{\left(\frac{dx(u)}{du}\right)^2+\left(\frac{dy(u)}{du}\right)^2}+y_0\right)du. \tag{3.27}$$

The first derivatives of the functions that describe Bezier curves are calculated according to the expressions [20]:

$$\frac{dx(u)}{du}=\sum_{k=1}^{n}x_kB'_{k,n}(u),\ \frac{dy(u)}{du}=\sum_{k=1}^{n}y_kB'_{k,n}(u). \tag{3.28}$$

Derivatives of Bernstein polynomials are calculated by the formula:

$$B'_{k,n}(u)=B_{k,n}(u)\frac{k-nu}{u(1-u)}, \tag{3.29}$$

In equations (3.27), $m_x$ and $m_x$ are linear limiting moments, which are determined by the formulas:

$$m_x=\frac{M_{Rd,fi,x}}{l_s},\ m_y=\frac{M_{Rd,fi,y}}{l_s}, \tag{3.30}$$

where $M_{Rd,fi,x}$ and $M_{Rd,fi,y}$ are the limiting moments of the panel fragments in the cell between the ribs of the reinforced concrete ribbed slab in orthogonal directions along the reinforcing bars. These moments are determined according to the recommendations of EN 1992-1-2, taking into account the reduction in the strength of reinforced concrete by the zone method. Then the obtained value is compared with the moment acting in the slab according to the calculation scheme. If the calculated value of the moment is greater, it means that the limit of fire resistance is not reached.

To determine the virtual work of external forces, the calculation scheme shown in **Fig. 3.19** is used.

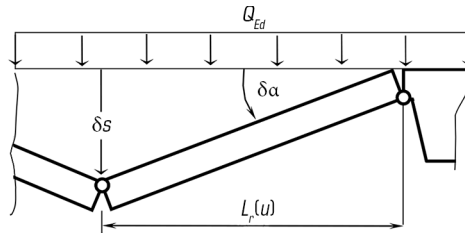


**Fig. 3.19** Scheme for determining possible movements when determining the work of external forces in the panel failure zone in the cell between the ribs of a reinforced concrete ribbed slab

Considering the schemes presented in **Fig. 3.16**, **3.18**, the elementary work of external forces for one symmetric quarter of the facet system at a certain point $A(x(u), y(u))$ in orthogonal directions is determined by the expressions:

$$dU_x = \frac{1}{2} Q_{Ed} \frac{dx(u)}{du} y(u),\ dU_C = \frac{1}{2} Q_{Ed} \frac{dC(u)}{du} E(u). \tag{3.31}$$

Taking into account formulas (3.31), the final formula for determining the virtual work of external forces of a symmetrical quarter of a mechanical system consisting of facets (**Fig. 3.16**) has the following form:

$$U = U_x + U_y,$$

$$U_x = \frac{1}{2} Q_{Ed} \int_0^1 \frac{dx(u)}{du} y(u) du,$$

$$U_y = \frac{1}{2} Q_{Ed} \int_0^1 \frac{dy(u)}{du} x(u) du. \tag{3.32}$$

To determine compliance with a given class of fire resistance, the corresponding condition should be checked, which has the following form:

$$W \geq U. \tag{3.33}$$

In this way, a simplified method of calculating the fire resistance of a reinforced concrete ribbed slab at the onset of the limit state of loss of integrity is proposed.

When implementing the algorithm for the calculated assessment of integrity according to the energy criterion, the scheme shown in **Fig. 3.20** can be used.

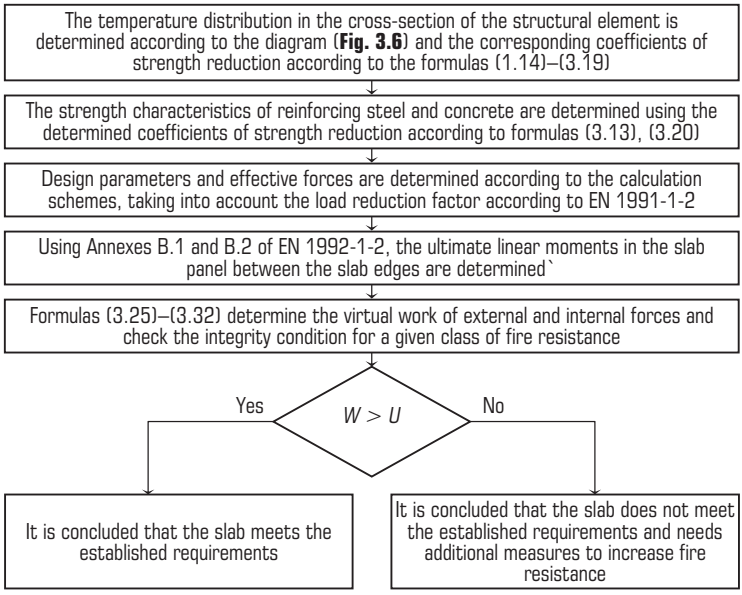


**Fig. 3.20** Scheme of the algorithm for the implementation of the method for the calculated assessment of the fire resistance of the reinforced concrete ribbed slab according to the limit state of the loss of integrity according to the energy criterion

The next step in the hierarchy of methods for calculating the fire resistance of reinforced concrete ribbed slabs based on the limit state of loss of integrity requires the use of refined methods. In [7] it was shown that these methods allow, based on the calculation results, to identify the moment of onset of the limit state of loss of integrity. To carry out the calculation according to this approach, a set of initial data is also required, which is presented in the form of a **Table 3.8**, basic mathematical models and theoretical references given in the **Tables 3.9**, **3.10** are also used for conducting.

When using the highest methods in the hierarchy, the algorithm of integration of mechanics equations by implicit and explicit methods is used. The algorithm of these methods can be implemented using the scheme presented in **Fig. 3.9**.

Thus, in **Fig. 3.10** the proposed hierarchical system of methods for calculation assessment of reinforced concrete hollow and ribbed slabs according to the limit state of loss of integrity is presented.

The proposed system of approaches to the assessment of fire resistance makes it possible to more accurately determine the fire resistance of structures using tabular, simplified or refined methods. This hierarchical system provides designers with choice at the design stage. If it is possible

to confirm the required class of fire resistance using the tabular method, the use of the simplified method can be avoided. In the case of a negative result, the designer can use a simplified method that takes into account the material, the cross-section of the structure and the load level, allowing to obtain more accurate indicators of fire resistance at the limit state of loss of integrity.

If the simplified method does not give the desired results, it is suggested to apply the refined method. This method more accurately determines the temperature distribution throughout the structure, allowing for a better assessment of concrete and reinforcement degradation, leading to even more accurate results compared to the simplified method.

## CONCLUSIONS

Summarizing the obtained results, it can be noted that the actual scientific and technical problem of substantiating the general hierarchical system of methods for calculating the fire resistance of reinforced concrete enclosing structures, in particular reinforced concrete hollow and ribbed slabs upon the onset of the limit state of loss of integrity during the thermal effect of the standard fire temperature regime, was solved. At the same time, the following main results were obtained:

1. The regularities of the onset of the limit state of loss of integrity of reinforced concrete hollow slabs during the thermal effect of the standard temperature regime of fire from their structural parameters were studied.

2. It was found that the studied regularity of the limit of fire resistance of reinforced concrete hollow slabs according to the loss of integrity from the height of the section ($H$) and the axial distance from the reinforcement to the heating surface of the slab ($w$) can be described using the regression dependence $U_e = 3.37 + 0.119H + 1.01w + 0.000625 \times H \times w$.

3. It was proved that the obtained regression dependence of the limit of fire resistance of reinforced concrete hollow slabs on their structural parameters allows obtaining adequate results, since the average error does not exceed 12 %.

4. On the basis of the obtained regularities, a nomogram was built to assess the fire resistance limit for reinforced concrete hollow slabs upon the onset of the limit state of loss of integrity.

5. A reference table was created for the assessed fire resistance of reinforced concrete hollow slabs based on the loss of integrity depending on the height of the section and the axial distance from the armature to the heating surface of the slab to justify the corresponding tabular method.

6. On the basis of the results obtained in this work and [5, 10], a hierarchical system of methods for calculating the calculation of reinforced concrete hollow slabs based on the onset of the limit state of loss of integrity was substantiated by creating algorithms for the implementation of simplified and refined methods substantiated in the work.

7. The regularities of the onset of the limit state of loss of integrity of reinforced concrete ribbed slabs during the thermal effect of the standard temperature regime of fire from their structural parameters were studied.

8. The regularity of the limit of fire resistance of reinforced concrete ribbed slabs based on the loss of integrity from the cross-sectional thickness of the panel between the ribs ($h_s$) and the axial distance from the reinforcement to the heating surface of the panel between the ribs ($w_s$) has been revealed and can be described using the regression dependence $U_e = 1.2 + 0.06h_s + 1.2w_s + 0.01 \times h_s \times w_s$.

9. It was proved that the obtained regression dependence of the limit of fire resistance of reinforced concrete ribbed slabs on their structural parameters allows obtaining adequate results, since the average error does not exceed 8 %.

10. On the basis of the obtained regularities, a nomogram was built to assess the fire resistance limit for reinforced concrete ribbed slabs upon the onset of the limit state of loss of integrity.

11. A reference table was created for the assessed fire resistance of reinforced concrete ribbed slabs based on the loss of integrity depending on the cross-section thickness of the panel between the ribs and the axial distance from the armature to the heating surface of the panel between the ribs of the slab to justify the appropriate tabular method.

12. Based on the results, in this work and in [6, 7], a hierarchical system of methods for calculating the assessed value of reinforced concrete ribbed slabs based on the onset of the limit state of loss of integrity was substantiated by creating algorithms for the implementation of simplified and refined methods substantiated in the work.

13. On the basis of the proposed approaches, a general hierarchical system of calculation methods for assessing the fire resistance of reinforced concrete hollow and ribbed slabs was created based on the onset of the limit state of loss of integrity.



## REFERENCES

1. Pozdieiev, S. V. (20212). Development of scientific basis for determination of fire endurance of bearing reinforced concrete structures [Doctoral dissertation; Instytut derzhavnoho upravlinnia u sferi tsyvilnoho zakhystu].
2. Kovalov, A. I. (2023). Development of the scientific basis of assessing the fire resistance of fireproof reinforced concrete building structures [Doctoral dissertation; Natsionalnyi universytet tsyvilnoho zakhystu Ukrainy Derzhavnoi sluzhby Ukrainy z nadzvychainykh sytuatsii].
3. Kovalov, A., Konoval, V., Khmyrova, A., Dudko, K. (2019). Parameters for simulation of the thermal state and fire-resistant quality of hollow-core floors used in the mining industry. E3S Web of Conferences, 123, 01022. https://doi.org/10.1051/e3sconf/201912301022
4. Sidnei, S., Nuianzin, V., Kostenko, T., Berezovskyi, A., Wąsik, W. (2023). A Method of Evaluating the Destruction of a Reinforced Concrete Hollow Core Slab for Ensuring Fire Resistance. Journal of Engineering Sciences, 10 (2), D1–D7. https://doi.org/10.21272/jes.2023.10(2).d1
5. Sidnei, S., Myroshnyk, O., Kovalov, A., Veselivskyi, R., Hryhorenko, K., Shnal, T., Matsyk, I. (2024). Identifying the evolution of through cracks in iron-reinforced hollow slabs under the

influence of a standard fire temperature mode. Applied Mechanics, 4 (7 (130)), 70–77. https://doi.org/10.15587/1729-4061.2024.310520
6. Sidnei, S., Berezovskyi, A., Kasiarum, S., Lytvynenko, O., Chastokolenko, I. (2023). Revealing patterns in the behavior of a reinforced concrete slab in fire based on determining its stressed and deformed state. Eastern-European Journal of Enterprise Technologies, 5 (7 (125)), 43–49. https://doi.org/10.15587/1729-4061.2023.289930
7. Тут будет ссылка с ВЕЖПТ за октябрь-2024.
8. Vasylkovskyi, O. M., Leshchenko, S. M., Vasylkovska, K. V., Petrenko, D. I. (2016). Pidruchnyk doslidnyka. Kirovohrad, 204.
9. Horvat, A. A., Molnar, O. O., Minkovych, V. V. (2019). Metody obrobky eksperymentalnykh danykh z vykorystanniam MS Excel. Uzhhorod: Vydavnytstvo UzhNU "Hoverla", 160.
10. Pozdieiev, S., Sidnei, S., Nekora, O., Subota, A., Kulitsa, O. (2023). Study of the Destruction Mechanism of Reinforced Concrete Hollow Slabs Under Fire Conditions. Smart Technologies in Urban Engineering, 447–457. https://doi.org/10.1007/978-3-031-46877-3_40
11. Wickström, U. (2016). Temperature Calculation in Fire Safety Engineering. Springer International Publishing. https://doi.org/10.1007/978-3-319-30172-3
12. S. Ma, S. Y. A., May, I. M. (1986). The Newton-Raphson method used in the non-linear analysis of concrete structures. Computers & Structures, 24 (2), 177–185. https://doi.org/10.1016/0045-7949(86)90277-4
13. Cremonesi, M., Franci, A., Idelsohn, S., Oñate, E. (2020). A State of the Art Review of the Particle Finite Element Method (PFEM). Archives of Computational Methods in Engineering, 27 (5), 1709–1735. https://doi.org/10.1007/s11831-020-09468-4
14. Rainone, L. S., Tateo, V., Casolo, S., Uva, G. (2023). About the Use of Concrete Damage Plasticity for Modeling Masonry Post-Elastic Behavior. Buildings, 13 (8), 1915. https://doi.org/10.3390/buildings13081915
15. Murray, Y. D., Abu-Odeh, A., Bligh, R. (2006). Evaluation of Concrete Material Model 159. FHWA-HRT-05-063.
16. Janssen, R. (2013). Fire Spalling of Concrete. Doctoral thesis in Concrete structures. Stockholm.
17. Pozdieiev, S., Nekora, O., Kryshtal, T., Sidnei, S., Shvydenko, A. (2019). Improvement of the estimation method of the possibility of progressive destruction of buildings caused by fire. IOP Conference Series: Materials Science and Engineering, 708 (1), 012067. https://doi.org/10.1088/1757-899x/708/1/012067
18. Pozdieiev, S., Nekora, O., Kryshtal, T., Zazhoma, V., Sidnei, S. (2018). Method of the calculated estimation of the possibility of progressive destruction of buildings in result of fire. MATEC Web of Conferences, 230, 02026. https://doi.org/10.1051/matecconf/201823002026
19. Vambersky, J. N. J. A. (1994). Precast concrete in buildings today and hi the future. The Structural Engineer, 72 (15).
20. Khern, D., Beiker, M. P. (2005). Kompiuternaia hrafyka y standart OpenGL. Moscow: Vyliams, 1168.